



Magneto-optical spectra and electron structure of $\text{Nd}_{0.5}\text{Gd}_{0.5}\text{Fe}_3(\text{BO}_3)_4$ single crystal



A.V. Malakhovskii^{a,*}, S.L. Gnatchenko^b, I.S. Kachur^b, V.G. Piryatinskaya^b, A.L. Sukhachev^a, V.L. Temerov^a

^a L. V. Kirensky Institute of Physics, Siberian Branch of Russian Academy of Sciences, 660036 Krasnoyarsk, Russian Federation

^b B. Verkin Institute for Low Temperature Physics and Engineering, National Academy of Sciences of Ukraine, 61103 Kharkov, Ukraine

ARTICLE INFO

Article history:

Received 18 August 2015

Accepted 20 October 2015

Available online 23 October 2015

PACS:

78.20.Ls

78.40.Ha

71.70.Ej

Keywords:

f-*f* transitions

Nd^{3+} ion

Magnetic circular dichroism

Electron structure

ABSTRACT

Polarized absorption spectra and magnetic circular dichroism (MCD) spectra of $\text{Nd}_{0.5}\text{Gd}_{0.5}\text{Fe}_3(\text{BO}_3)_4$ single crystal were measured in the range of 10000–21000 cm^{-1} and at temperatures 2–300 K. On the basis of these data, in the paramagnetic state of the crystal, the *4f* states of the Nd^{3+} ion were identified in terms of the irreducible representations and in terms of $|J, \pm M_J\rangle$ wave functions of the free atom. The changes of the Landé factor during *f*-*f* transitions were found theoretically in the $|J, \pm M_J\rangle$ wave functions approximation and were determined experimentally with the help of the measured MCD spectra. In the majority of cases the experimentally found values are close to the theoretically predicted ones.

© 2015 Elsevier B.V. All rights reserved.

1. Introduction

The family of the rare-earth (RE) borates with the common formula $\text{RM}_3(\text{BO}_3)_4$, where $M=\text{Al, Ga, Fe, Cr, Sc}$ and R – RE element, attracts considerable interest both in the fundamental aspect and in view of their manifold potential applications. In particular, the alumborates possess the very good luminescent and nonlinear optical properties and can be used in the mini-lasers and in the lasers with the self-doubling frequency [1–3]. The growing interest to the RE ferrobates $\text{RFe}_3(\text{BO}_3)_4$ during the last years is stimulated by discovering of the multiferroic properties (i.e. correlation between magnetic, elastic and electric ordering) in many of them [4–8]. The multiferroic effects open the possibility of these materials usage in new multifunctional devices with the mutual control of magnetic, electric and elastic characteristics.

At high temperatures the RE ferrobates crystallize in the trigonal huntite-like structure with the space group $R\bar{3}2 (D_3^d)$ [9–11]. The unit cell contains three formula units. The RE ions are located at the centers of the trigonal prisms RO_6 (the D_3 symmetry positions). The Fe^{3+} ions occupy the C_3 positions in the octahedral environment of oxygen ions; these octahedrons form helicoidal

chains along the C_3 axis. With the lowering temperature, some ferrobates with small ionic radius of RE ions undergo a structural phase transition to the $P3_121 (D_3^d)$ symmetry phase [11]. It results in reducing of the RE ion position symmetry to the C_2 one and in appearance of two nonequivalent positions of Fe^{3+} ions (C_2 and C_1).

Magnetic phase transitions in the mixed borates $\text{Nd}_x\text{Gd}_{1-x}\text{Fe}_3(\text{BO}_3)_4$ were studied by the optical spectroscopy method in Ref. [12]. It was found out that both the Neel temperature and the spin-reorientation transition temperature increase with the growth of the Nd concentration. The $\text{Nd}_{0.5}\text{Gd}_{0.5}\text{Fe}_3(\text{BO}_3)_4$ crystal, the same as the pure Nd and Gd ferrobates, reveals multiferroic properties [13]. Magnetic properties of the crystal $\text{Nd}_{0.5}\text{Gd}_{0.5}\text{Fe}_3(\text{BO}_3)_4$ were studied in Ref. [14]. It was shown that below the $T_N=32$ K it has an easy-plane AFM structure and the spin-reorientation does not occur down to 2 K. Any structural phase transitions were also not found down to 2 K.

Optical spectra of the Nd^{3+} ion in the $\text{NdFe}_3(\text{BO}_3)_4$ crystal in a wide spectral range (1500–25000 cm^{-1}) were studied in Ref. [15] and the crystal-field parameters and *g*-factors of the Nd^{3+} states were calculated. The first measurements of the optical absorption spectra of the $\text{Nd}_{0.5}\text{Gd}_{0.5}\text{Fe}_3(\text{BO}_3)_4$ single crystal at temperatures 90–300 K as well as their analysis with the help of the Judd-Ofelt theory were performed in Ref. [16]. Some results of study of the

* Corresponding author. Fax: +7 391 2438923.

E-mail address: malakha@iph.krasn.ru (A.V. Malakhovskii).

optical and magneto-optical properties of the $\text{Nd}_{0.5}\text{Gd}_{0.5}\text{Fe}_3(\text{BO}_3)_4$ crystal were presented in Refs. [17,18]. A number of peculiarities of the selection rules for electron transitions in the magnetically ordered state of the crystal as well as the specific features of the local environment of the excited Nd^{3+} ions were found.

In the present work, the magnetic circular dichroism (MCD) and absorption spectra of f - f transitions from 11000 cm^{-1} till the edge of the strong absorption at $\sim 22000\text{ cm}^{-1}$ are investigated. The crystal field split components of the $4f$ states are identified on the basis of the absorption and MCD spectra. The MCD spectra allow finding not only the symmetry of the states but also their origin from the states of $|J, \pm M_J\rangle$ type of the free ion, and allow finding the change of the Landé factor during f - f transitions.

2. Experimental details

$\text{Nd}_{0.5}\text{Gd}_{0.5}\text{Fe}_3(\text{BO}_3)_4$ single crystals were grown from the melt solution on the base of $\text{K}_2\text{Mo}_3\text{O}_{10}$ as described in Ref. [19]. At room temperature, the crystal has lattice constants: $a = 9.557(7)\text{ \AA}$ and $c = 7.62(1)\text{ \AA}$ [14]. The absorption spectra were measured with the light propagating normal to the C_3 axis of the crystal for the light electric vector \vec{E} parallel (the π spectrum) and perpendicular (the σ spectrum) to the C_3 axis and the light propagating along the C_3 axis (the α spectrum). The spectral resolution at the low temperature measurements was approximately equal to 1.5 cm^{-1} . The absorption spectra measured in the σ and α polarizations coincide with each other within the limit of the experimental error. This implies that the absorption mainly occurs through the electric dipole mechanism.

At $T = 2\text{ K}$ the sample was placed in the liquid helium. For the measurements of absorption spectra at $T > 4.2\text{ K}$ a liquid-helium cooled cryostat was used. It had an internal volume filled by the gaseous helium where the sample was placed.

The MCD was measured in the field 5 kOe by the light-polarization modulation method using a piezoelectric modulator (details are in Ref. [20].) The spectral resolution of the MCD measurements was $\sim 10\text{ cm}^{-1}$ and sensitivity was 10^{-4} . The MCD measurements were carried out in α -polarization with the sample positioned in the gas flow cryostat.

3. Background for characterization of electronic transitions and states.

Electron states in crystals are characterized by the irreducible representations in the group of the local symmetry (D_3 in our case). These characteristics of the states are found from polarization of transitions and from selection rules of Table 1. In crystals of the axial symmetry the electron states have one more characteristic: the crystal quantum number μ . In trigonal crystals it has values [21]: $\mu = +1/2, -1/2, 3/2 (\pm 3/2)$. Additionally, in the axial crystals the electron states can be described in a first approximation by $|J, \pm M_J\rangle$ wave functions of the free atom. Between values of μ and M_J there is the following correspondence [21]:

$$M_J = \pm 1/2, \pm 3/2, \pm 5/2, \pm 7/2, \pm 9/2, \pm 11/2, \pm 13/2$$

$$\mu = \pm 1/2, (\pm 3/2), \mp 1/2, \pm 1/2, (\pm 3/2), \mp 1/2, \pm 1/2 \quad (1)$$

Table 1
Selection rules for electric dipole transitions in D_3 symmetry.

	$E_{1/2}$	$E_{3/2}$
$E_{1/2}$	$\pi, \sigma(\alpha)$	$\sigma(\alpha)$
$E_{3/2}$	$\sigma(\alpha)$	π

The states with $\mu = \pm 1/2$ correspond to the $E_{1/2}$ states and the states with $\mu = (\pm 3/2)$ correspond to the $E_{3/2}$ states in the D_3 group notations. Selection rules for the number μ in crystals are similar to those for the number M_J in free atoms [21]. For the electric dipole absorption

$$\Delta\mu = \pm 1 \text{ corresponds to}$$

$$\mp \text{ circularly polarized and } \sigma\text{-polarized waves,}$$

$$\Delta\mu = 0 \text{ corresponds to } \pi\text{-polarized waves.} \quad (2)$$

For the linearly polarized waves, these selection rules coincide, of course, with that of Table 1.

According to the definition, the splitting of the Kramers doublets in the magnetic field directed along the C_3 axis of a crystal is:

$$\Delta E = \mu_B g_C H. \quad (3)$$

Here g_C is the effective Landé factor in the C_3 -direction. The same value in the approximation of the $|J, \pm M_J\rangle$ function is evidently defined by the equation:

$$\Delta E = 2g\mu_B M_J H, \quad (4)$$

where g is the Landé factor of the free atom. Correspondingly, the Landé factor of the Kramers doublet along the C_3 axis in the same approximation is

$$g_{CM} = 2gM_J \quad (5)$$

These values for the states of Nd^{3+} ion are given in Table 2. The states with the same μ and different M_J (see Eq. (1)) can mix in the crystal, and the resulting g_C can differ from g_{CM} . The prevailing M_J state of the free atom in the crystal field state can be found in a first approximation (Table 3) basing on the comparison of g_{CM} for the corresponding M_J (Table 2) with the theoretical g_C in the $\text{NdFe}_3(\text{BO}_3)_4$ crystal (Table 3). The MCD spectra can help to identify states in the $|J, \pm M_J\rangle$ functions approximation and to find the Zeeman splitting of lines.

The MCD conditioned by a pair of the Zeeman splitting components is evidently described by the equation:

$$\Delta k = k_{m+}\phi(\omega, \omega_0 + \Delta\omega_0) - k_{m-}\phi(\omega, \omega_0 - \Delta\omega_0) \quad (6)$$

Here k_+ and k_- are the amplitudes of (+) and (−) circularly polarized lines, ϕ are the form functions of (+) and (−) polarized lines. If the Zeeman splitting $\Delta\omega_0$ is much less than the line width, then one obtains

$$\Delta k = k_m c \phi(\omega, \omega_0) + k_m \Delta\omega_0 \partial\phi(\omega, \omega_0) / \partial\omega_0. \quad (7)$$

Here $k_m = k_{m+} + k_{m-}$ is amplitude of the line not split by the magnetic field and $c = (k_{m+} - k_{m-}) / k_m$. The first term in (7) is the paramagnetic MCD and the second one is the diamagnetic MCD.

Table 2
Landé factors of the Kramers doublets along the C_3 axis of a crystal in approximation of the $|J, \pm M_J\rangle$ functions.

	M	13/2	11/2	9/2	7/2	5/2	3/2	1/2
$^4I_{9/2}, g = 0.727$	g_{CM}			6.54	5.09	3.64	2.18	0.727
$^4F_{3/2}, g = 0.4$	g_{CM}						1.2	0.4
$^4F_{5/2}, g = 1.029$	g_{CM}					5.14	3.09	1.03
$^2H_{9/2}, g = 0.909$	g_{CM}			8.18	6.36	4.55	2.73	0.909
$^4S_{3/2}, g = 2$	g_{CM}						6	2
$^4F_{7/2}, g = 1.238$	g_{CM}				8.67	6.19	3.71	1.238
$^4G_{5/2}, g = 0.571$	g_{CM}					2.855	1.713	0.571
$^2G_{7/2}, g = 0.889$	g_{CM}				6.223	4.445	2.667	0.889
$^4G_{7/2}, g = 0.984$	g_{CM}				6.888	4.92	2.952	0.984
$^4G_{9/2}, g = 1.1717$	g_{CM}			10.54	8.202	5.86	3.515	1.1717
$^2K_{13/2}, g = 0.933$	g_{CM}	12.1	10.27	8.4	6.53	4.66	2.8	0.933

Table 3Parameters of transitions and states. Energies of transitions (E) are given at 40 K. (Details are in the text).

State	Level	$E \text{ cm}^{-1}$	Polar.	Sym.	μ	M_J	Δg_C (exp)	Δg_{CM}	g_{\perp} [15]	g_C [15]	g_{CM}
$^4I_{9/2}$	Gr1	0	–	$E_{1/2}$	$\mp 1/2$	$\pm 5/2$			2.385	1.376	3.64
	Gr2	~ 78	–	$E_{3/2}$	$3/2$	$\pm 9/2$			0	3.947	6.54
	Gr3	150	–	$E_{1/2}$	$\pm 1/2$	$\pm 7/2$			2.283	2.786	5.09
	Gr4	220	–	$E_{3/2}$	$3/2$	$\pm 3/2$			0	3.879	2.18
	Gr5		–	$E_{1/2}$	$\pm 1/2$	$\pm 1/2$			3.527	0.843	0.727
$^4F_{3/2}$	R1	11369	π, σ	$E_{1/2}$	$\pm 1/2$	$\pm 1/2$	(+)	+3.24	0.926	0.251	0.4
	R2	11436	σ	$E_{3/2}$	$3/2$	$\pm 3/2$	–3.4	–4.84	0	1.562	1.2
$^4F_{5/2}$	S1	12382	π, σ	$E_{1/2}$	$\pm 1/2$	$\pm 1/2$	(–)	+2.61	3.158	0.598	1.03
	S2	12450	π, σ	$E_{1/2}$	$\mp 1/2$	$\pm 5/2$	+8.4	+8.78	0.096	4.713	5.14
	S3	12467	σ	$E_{3/2}$	$3/2$	$\pm 3/2$	(–)	–6.73	0	2.576	3.09
$^2H_{9/2}$	S4	12495	π, σ	$E_{1/2}$	$\pm 1/2$	$\pm 7/2$	–3.3	–2.72	1.989	4.633	6.36
	S5	12553	π, σ	$E_{1/2}$	$\pm 1/2$	$\pm 1/2$		+2.73	3.995	0.982	0.909
	S6	12578	σ	$E_{3/2}$	$3/2$	$\pm 3/2$		–6.37	0	2.169	2.73
	S7	12620	π, σ	$E_{1/2}$	$\mp 1/2$	$\pm 5/2$	+4.9	+8.19	2.877	2.765	4.55
	S8	12702	σ	$E_{3/2}$	$3/2$	$\pm 9/2$	+13.9	–11.8	0	7.788	8.18
$^4F_{7/2}$	A1	13353	π, σ	$E_{1/2}$	$\pm 1/2$	$\pm 1/2$		+2.4	3.216	0.673	1.238
	A2	13370	σ	$E_{3/2}$	$3/2$	$\pm 3/2$	–8.6	–7.35	0	3.524	3.71
	A3		$\pi, (\sigma?)$	$E_{1/2}$	$\mp 1/2$	$\pm 5/2$		+9.83	4.895	1.296	6.19
	A4		$(\pi?)\sigma$	$E_{1/2}$	$\pm 1/2$	$\pm 7/2$		–5.03	3.858	2.141	8.67
$^4S_{3/2}$	A5	13488	π, σ	$E_{1/2}$	$\pm 1/2$	$\pm 1/2$		+1.64	3.239	1.884	2
	A6	13499	σ	$E_{3/2}$	$3/2$	$\pm 3/2$	–7.55	–9.64	0	5.848	6
$^4G_{5/2}$	D1	16921	π, σ	$E_{1/2}$	$\pm 1/2$	$\pm 1/2$	(+)	+3.07	0.043	0.065	0.571
	D2	17062	π, σ	$E_{1/2}$	$\mp 1/2$	$\pm 5/2$	(+)	+6.5	1.385	1.310	2.885
	D3	17100	$\approx \sigma$	$E_{3/2}$	$3/2$	$\pm 3/2$	(–)	–5.35	0	3.044	1.713
$^2G_{7/2}$	D4	17199	π, σ	$E_{1/2}$	$\pm 1/2$	$\pm 1/2$	(–)	+2.75	2.617	0.266	0.889
	D5	17240	π, σ	$E_{1/2}$	$\pm 1/2$	$\pm 7/2$	(+)	–2.58	0.755	3.308	6.223
	D6	17289	π, σ	$E_{1/2}$	$\mp 1/2$	$\pm 5/2$	(–)	+8.08	1.538	0.954	4.445
	D7	17325	$\approx \sigma$	$E_{3/2}$	$3/2$	$\pm 3/2$	(–)	–6.31	0	1.016	2.667
$^4G_{9/2}$	E1	18872	π, σ	$E_{1/2}$	$\pm 1/2$	$\pm 7/2$	(–)	+2.47	3.369	1.784	1.17
	E2	18910	π, σ	$E_{1/2}$	$\mp 1/2$	$\pm 5/2$	(–)	+9.5	2.098	3.026	5.86
	E3	18959	$\approx \sigma$	$E_{3/2}$	$3/2$	$\pm 3/2$	(–)	–7.17	0	2.924	3.515
	E4	19010	π, σ	$E_{1/2}$	$\pm 1/2$	$\pm 1/2$		–4.56	2.292	2.081	8.202
	E5	19064	σ	$E_{3/2}$	$3/2$	$\pm 9/2$		–14.2	0	8.530	10.54
$^2K_{13/2}$ + $^4G_{7/2}$	F1	19295	π, σ	$E_{1/2}$	$\mp 1/2$	$\pm 11/2$	+10.7	+13.9	0.283	9.760	10.27
	F2	19323	π, σ	$E_{1/2}$							
	F3	19389	π, σ	$E_{1/2}$							
	F4	19408	π, σ	$E_{1/2}$							
	F5	19438	π, σ	$E_{1/2}$							
	F6	19461	σ	$E_{3/2}$	$3/2$	$\pm 9/2$	+8.8	–12.0	0	7.030	8.4
	F7	19525	π, σ	$E_{1/2}$			(–)				
	F8	19687	π, σ	$E_{1/2}$							
	F9	19769	σ	$E_{3/2}$	$3/2$	$\pm 3/2(G)$	(–)	–6.6	0	3.025	2.952
	F10	19793	π, σ	$E_{1/2}$							

The fine structure of the MCD spectra is conditioned by the diamagnetic effect. The Zeeman splitting of an absorption line $2\Delta\omega_0$ is found through the Zeeman splitting of the initial and final levels (the Kramers doublets in particular):

$$2\hbar\Delta\omega_0 = \pm (\Delta E_i \pm \Delta E_f) = \mu_B H \Delta g_C. \quad (8)$$

The sign of the temperature dependent paramagnetic effect (c in Eq. (7)) is defined by polarization of the transition from the lower component of the Zeeman splitting of the initial state. Sign of the diamagnetic effect ($\Delta\omega_0$ in Eq. (7)) is not so unambiguous. The first sign in (8) is the sign of the paramagnetic effect and the second one indicates that the splitting of the line can be sum or difference of the splitting of the initial and final states (see below).

The MCD spectra allow us to find the Zeeman splitting of lines

and, consequently, the change of the Landé factor during the electron transition. In the case of the Gaussian shape of the absorption line, the Zeeman splitting is found with the help of the formula [22]:

$$\Delta\omega_0 = \frac{\Delta k_{dm}}{k_m} |\omega_m - \omega_0| \sqrt{e}. \quad (9)$$

Here values Δk_{dm} and ω_m are amplitude and position of extremum of the diamagnetic MCD, respectively, k_m is amplitude of the α -polarized absorption line. For the Lorentzian form function \sqrt{e} should be replaced by “2”. Formula (9) can, evidently, be used only for the solitary, well resolved pair of the Zeeman splitting components.

The general schematic diagram of the $4f$ states and f -

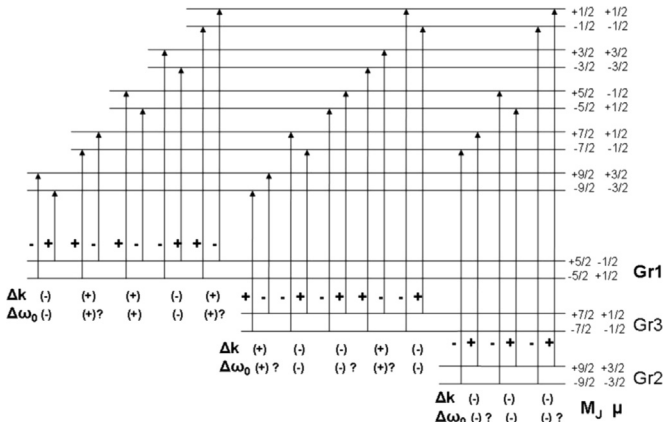


Fig. 1. General scheme of f - f transitions in Nd^{3+} ion.

transitions and their circular polarizations in the magnetic field directed along the C_3 axis (see Fig. 1) can be created with the help of (1) and (2), taking into account in a first approximation the splitting (4) in the magnetic field according to $\pm M_J$ and the splitting in the crystal field (CF) according to $|M_J|$. The real positions of states with the different values of the M_J will be found below on the basis of the experimental data analysis. When the splitting of an absorption line in the magnetic field is equal to the difference of the splitting of the states (sign minus in (8) in brackets) and these splitting are close in value, the supposed sign of the line splitting is not definite.

4. Results and discussion

Absorption spectra of the $\text{Nd}_{0.5}\text{Gd}_{0.5}\text{Fe}_3(\text{BO}_3)_4$ crystal consist of the narrow bands corresponding to f - f transitions in Nd^{3+} ions and of the wide bands due to d - d transitions in Fe^{3+} ions [18]. The d - d spectra were subtracted from the total spectra and so the f - f spectra were obtained (Fig. 2). From the high energy side the studied spectra are restricted by the strong absorption conditioned by the Fe ions [18]. The f - f bands were identified according to Ref. [23]. Symbols of absorption bands (Fig. 2) were given according to Ref. [24]. Absorption spectra of the f - f transitions were measured in the temperature range of 2–300 K and the MCD spectra were measured in the temperature range 90–300 K. The MCD

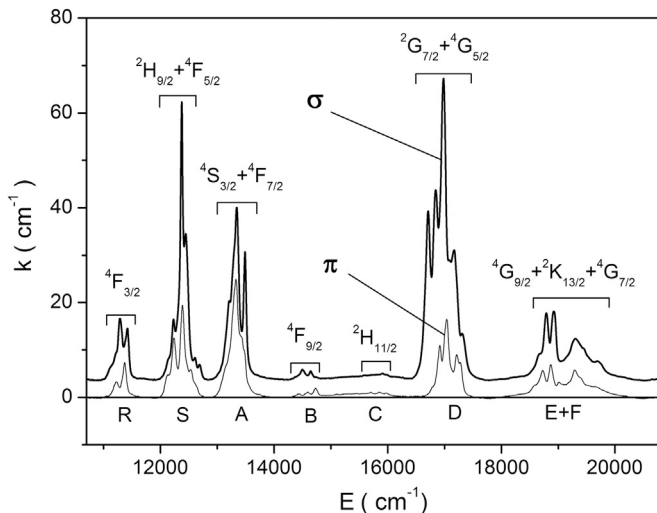


Fig. 2. Polarized absorption spectra of the f - f transitions in $\text{Nd}_{0.5}\text{Gd}_{0.5}\text{Fe}_3(\text{BO}_3)_4$ crystal at room temperature. The final states of the Nd^{3+} ion are indicated.

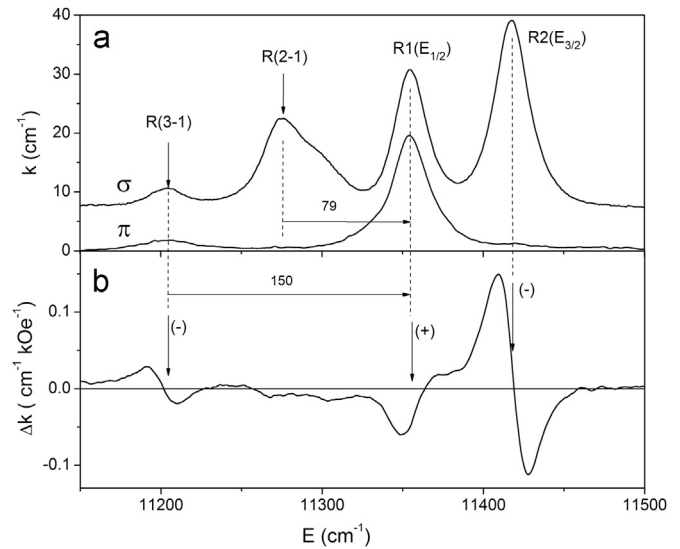


Fig. 3. Polarized absorption spectra (a) and MCD spectra (b) of the ${}^4I_{9/2} \rightarrow {}^4F_{3/2}$ transition (R-band) at $T=90$ K.

conditioned by the d - d transitions was not observed, and all the measured MCD spectra are due to the f - f transitions. The absorption and MCD spectra were studied for the R, S, A, D and (E+F) bands (see Fig. 2). The detailed absorption and MCD spectra of the f - f transitions will be given below.

4.1. ${}^4I_{9/2} \rightarrow {}^4F_{3/2}$ transition (R band)

Preliminary results concerning the R band were presented in Ref. [18]. The polarized absorption and MCD spectra of the transition ${}^4I_{9/2} \rightarrow {}^4F_{3/2}$ are depicted in Fig. 3. At the liquid helium temperature only lines R1 and R2 are observed in the R band. According to the polarization of these lines and selection rules of Table 1, the symmetry of the lowest level of the ground multiplet (Gr1) is $E_{1/2}$ and symmetries of the levels R1 and R2 are $E_{1/2}$ and $E_{3/2}$, respectively (Table 3). The R(2-1) and R(3-1) lines (Fig. 3) correspond to the transitions from the levels Gr2 and Gr3 at the energies 79 and 150 cm^{-1} , respectively, to the R1 state (Table 3). From the polarization of the R(2-1) and R(3-1) lines and from the selection rules of Table 1 it follows that the Gr2 and Gr3 levels have symmetries $E_{3/2}$ and $E_{1/2}$, respectively (Table 3). The R(2-1) line can be identified also as the transition $\text{Gr3} \rightarrow \text{R2}$ according to its position and the selection rules. However, the temperature dependencies of the R(2-1) and R(3-1) lines intensities testify that the former assumption is more correct.

Signs of the diamagnetic MCD (signs of $\Delta\omega_0$) are easily found from Fig. 3 according to the definition (6) (they are shown in Fig. 3 and Table 3). There are at least two suitable candidates for the ground state with $E_{1/2}$ symmetry: $M_J = \pm 7/2$ ($\mu = \pm 1/2$) and $M_J = \pm 5/2$ ($\mu = \mp 1/2$) (Fig. 1). However, according to Fig. 1, only in the case of the ground state $M_J = \pm 5/2$ ($\mu = \mp 1/2$) the diamagnetic MCD of lines R1 and R2 has experimentally observed signs (Fig. 3). Despite the trigonal symmetry of the $\text{Nd}_{0.5}\text{Gd}_{0.5}\text{Fe}_3(\text{BO}_3)_4$ crystal, it has the easy plane magnetic anisotropy in the magnetically ordered state [14], i. e., the crystallographic single axial anisotropy is not strong. As a consequence, the order of the levels and their Landé factors can not correspond to the value of the magnetic quantum number M_J of the free atom. The Gr3 level (Table 3, Fig. 1) can be referred to the state $M_J = \pm 7/2$ ($\mu = \pm 1/2$). Indeed, according to Fig. 1, the transitions from the level $M_J = 7/2$ should have opposite circular polarizations relative to those of the transitions from the lowest level $M_J = 5/2$, and the line R(3-1) ($\text{Gr3} \rightarrow \text{R1}$ transition) should have negative diamagnetic MCD ($\Delta\omega_0 < 0$), that

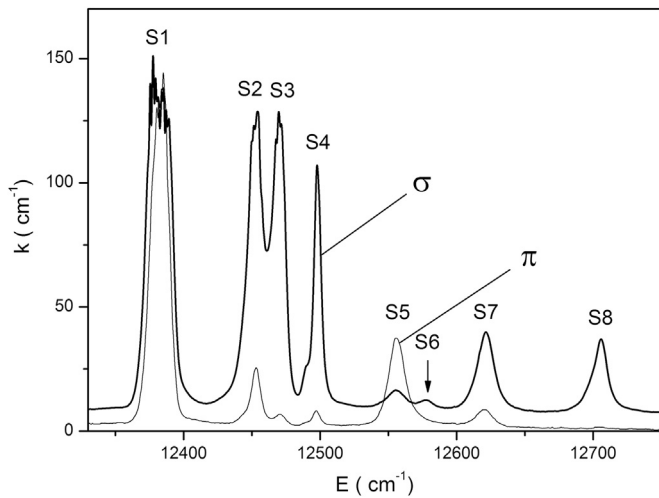


Fig. 4. Polarized absorption spectra of the ${}^4I_{9/2} \rightarrow {}^2H_{9/2} + {}^4F_{5/2}$ transitions (S-band) at $T=6$ K.

is really observed (Fig. 3). The R(2-1) line (Gr2 \rightarrow R1 transition) should have positive diamagnetic effect. This absorption line has asymmetric shape (Fig. 3). The most probably, it is due to the vibronic sideband which can have the diamagnetic MCD of the opposite sign relative to that of the electronic origin. This can be the reason of the small MCD of the R(2-1) line (Fig. 3). Some lines in the D band have the similar shape (see below).

With the help of the procedure described above, the Zeeman splitting of the R2 line (in the field $H=1$ kOe) was found: $2\Delta\omega_0 = -0.16$ cm^{-1} and the corresponding change of the Landé factor is: $\Delta g_C = -3.4$ (Table 3). Since Δg_C is proportional to $\Delta\omega_0$ we ascribe sign of $\Delta\omega_0$ to Δg_C . According to (8), diagram of Fig. 1 and Table 2 the change of the Landé factor in the $|J, \pm M_J\rangle$ function approximation is: $\Delta g_{CM} = -(1.2 + 3.64) = -4.84$ (Table 3). Sum of the absolute values of the theoretical g_C in $\text{NdFe}_3(\text{BO}_3)_4$ (Table 3) for this transition is 2.938.

4.2. ${}^4I_{9/2} \rightarrow {}^2H_{9/2} + {}^4F_{5/2}$ transitions (S band)

Excited state of the S transition is split in the following way: ${}^4F_{5/2}$: $2E_{1/2} + E_{3/2}$ and ${}^2H_{9/2}$: $3E_{1/2} + 2E_{3/2}$. Symmetries of states in

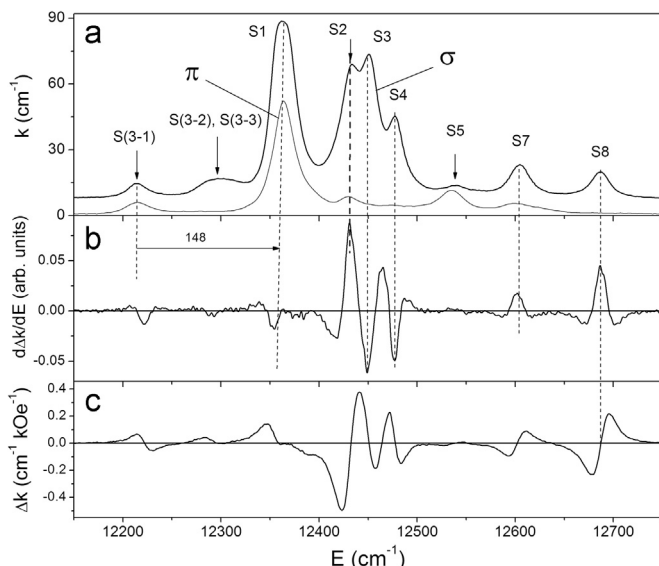


Fig. 5. Polarized absorption spectra (a), the first derivative of MCD (b) and MCD spectra (c) of the ${}^4I_{9/2} \rightarrow {}^2H_{9/2} + {}^4F_{5/2}$ transitions (S-band) at $T=90$ K.

the S manifold (Table 3) are found according to the linear polarizations of the absorption lines (Fig. 4), selection rules of Table 1 and above identification of the ground state. Signs of the Zeeman splitting $\Delta\omega_0$ of lines in the S band are not so much evident from the MCD spectra (Fig. 5) as in the R band. It is possible to show [22] that signs of extremums of the $\partial\Delta k/\partial\omega$ function at the absorption line positions give signs of the diamagnetic effect (see Fig. 5 and Table 3). The prevailing M_J states of the free atom in the crystal field states of the S manifold (Table 3) can be preliminary found basing on the comparison of the Landé factors g_{CM} for the corresponding M_J with the theoretical g_C in the $\text{NdFe}_3(\text{BO}_3)_4$ crystal (Tables 3 and 2). They are of course different but the succession of the values permits us to identify the origin of the S states from the M_J states.

The genetic origination of the crystal field states from the M_J states of the free atom on the ground of the diamagnetic MCD signs is not unambiguous for this manifold. According to the diagram of Fig. 1, the transitions $E_{1/2} (M=5/2) \rightarrow E_{3/2}$ (S3, S6 and S8 lines) can have only negative signs of the diamagnetic MCD but in the S8 line it is positive (Fig. 5, Table 3). Additionally, the lines S(3-1) and S1 should have opposite signs of the diamagnetic effect, the same as it takes place for R(3-1) and R1 lines (see above). However, the lines S(3-1) and S1 have diamagnetic effects of the same sign (Fig. 5). The Zeeman splitting $2\Delta\omega_0$ of lines S2, S4, S7 and S8 were found as described above. They are: $+0.39$, -0.154 , $+0.23$ and $+0.647$ cm^{-1} , respectively. Corresponding changes of the Landé factors are given in Table 3. The theoretical changes of the Landé factors in the $|J, \pm M_J\rangle$ function approximation were calculated according to the identification of the M_J value of the excited states (Table 3), diagram of Fig. 1 and Eq. (8). Comparison of the theoretical Δg_{CM} with the measured ones permitted us to refine identification of the S4 and S5 states (see Table 3). The theoretical value for S8 line is close in absolute value to the experimental one but have the opposite sign.

4.3. ${}^4I_{9/2} \rightarrow {}^4S_{3/2} + {}^4F_{7/2}$ transitions (A band)

Absorption spectra of the A band at 2 K are shown in Fig. 6. The excited state is split in the following way: ${}^4S_{3/2}$: $E_{1/2} + E_{3/2}$ and ${}^4F_{7/2}$: $3E_{1/2} + E_{3/2}$. Quantity of the observed lines corresponds to this splitting. Assignment of A1, A2, A5 and A6 states based on the polarizations of the corresponding lines (Fig. 6) is unambiguous. Polarization of the A3 and A4 lines is not evident, but there is no other possibility for their assignment as shown in Table 3.

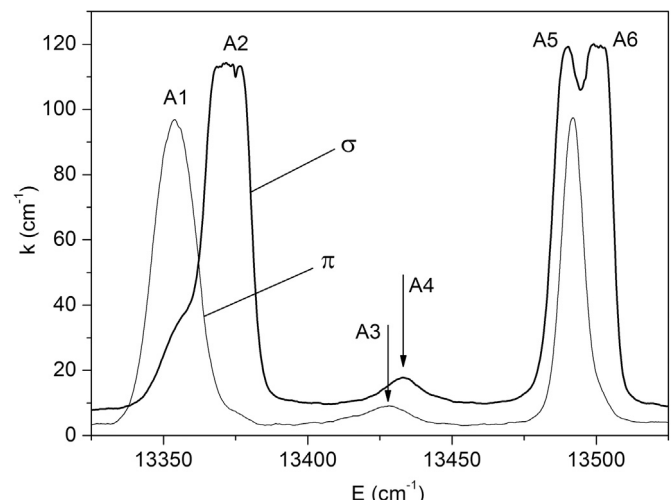


Fig. 6. Polarized absorption spectra of the ${}^4I_{9/2} \rightarrow {}^4S_{3/2} + {}^4F_{7/2}$ transitions (A-band) at $T=2$ K.

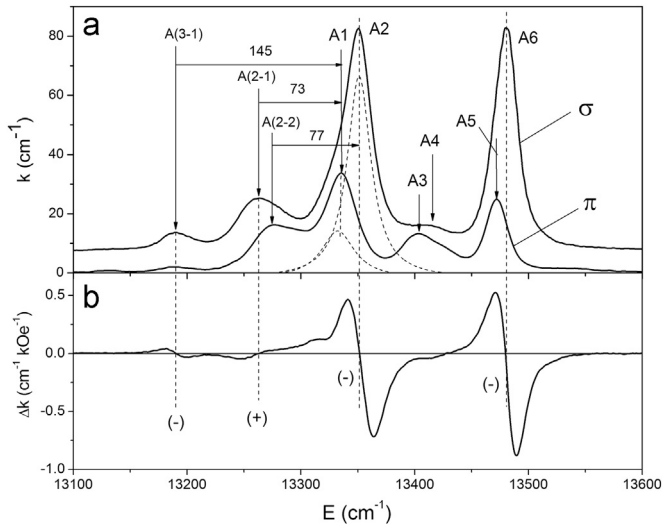


Fig. 7. Polarized absorption spectra (a) and MCD spectra (b) of the ${}^4I_{9/2} \rightarrow {}^4S_{3/2} + {}^4F_{7/2}$ transitions (A-band) at $T=90$ K.

Origination of the A states from the $|J, \pm M_J\rangle$ states was supposed, comparing the theoretical values of g_C in $\text{NdFe}_3(\text{BO}_3)_4$ with g_{CM} (Table 3). Large difference between these values for the A3 and A4 states is surprising. Probably it is connected with the not strong axial anisotropy and, as a consequence, with the large value of g_{\perp} (Table 3). The A1 and A5 lines are very weak in the σ -polarization at 90 K (Fig. 7), therefore they give very small contribution into the MCD, and practically all MCD is due to A2 and A6 lines (Fig. 7). The Zeeman splitting and corresponding Δg_C for these transitions were found as described above (see Table 3). Values of Δg_{CM} were also calculated (Table 3). Observed Δg_C are close to Δg_{CM} and their signs correspond to the identification according to the diagram of Fig. 1. The assignment of transitions from the upper sublevels of the ground state (Fig. 7) corresponds to their linear polarizations.

4.4. ${}^4I_{9/2} \rightarrow {}^4G_{5/2} + {}^2G_{7/2}$ transitions (D band)

Excited state of the D manifold is split in the following way: ${}^4G_{5/2}: 2E_{1/2} + E_{3/2}$ and ${}^2G_{7/2}: 3E_{1/2} + E_{3/2}$. Symmetries of states in the D manifold are found (Table 3) according to the linear polarizations of the absorption lines (Fig. 8, Table 3), selection rules of Table 1 and above identification of the ground state. Signs of the

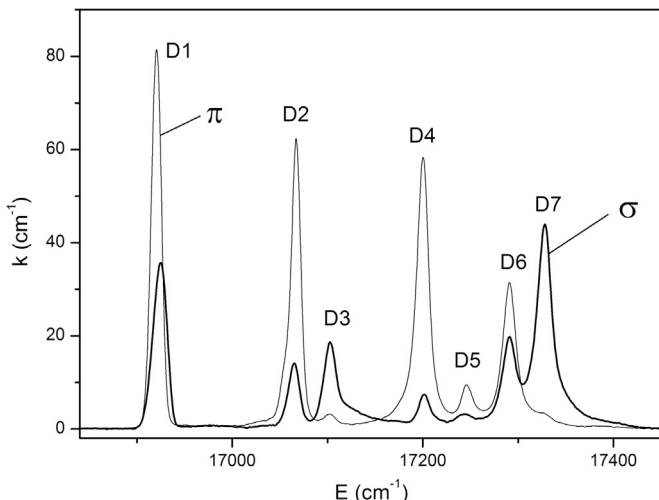


Fig. 8. Polarized absorption spectra of the ${}^4I_{9/2} \rightarrow {}^4G_{5/2} + {}^2G_{7/2}$ transitions (D-band) at $T=6$ K.

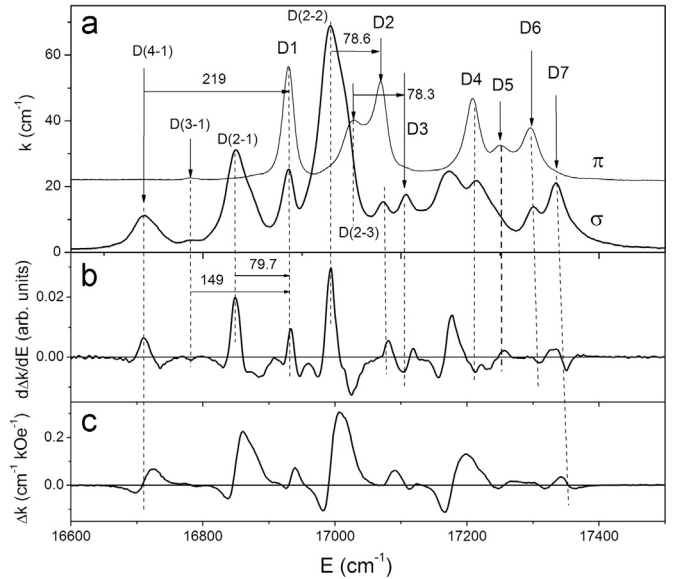


Fig. 9. Polarized absorption spectra (a), the first derivative of MCD (b) and MCD spectra (c) of the ${}^4I_{9/2} \rightarrow {}^4G_{5/2} + {}^2G_{7/2}$ transitions (D-band) at $T=90$ K.

circular polarizations of the lines (Table 3) were found with the help of the first derivative of the MCD spectrum (Fig. 9). Unfortunately, it was possible to find the Zeeman splitting $\Delta\omega_0$ and corresponding $\Delta g_C = +5.6$ only for D(4-1) transition (Fig. 9) from the Gr4 sublevel of the ground state (Table 3). σ -polarization of this line permitted to identify symmetry of the Gr4 state as $E_{3/2}$ (see Table 3). According to the identification of the D(4-1) transition, $\Delta g_{CM} = -1.61$ for it. Shapes of D(2-1) and D(2-2) lines (Fig. 9) are similar to that of the R(2-1) line (Fig. 3) and probably they are also due to the vibronic side-bands.

4.5. ${}^4I_{9/2} \rightarrow {}^4G_{9/2} + {}^4G_{7/2} + {}^2K_{13/2}$ transitions (E+F bands)

Excited state of the (E+F) manifold is split in the following way: ${}^4G_{9/2}: 3E_{1/2} + 2E_{3/2}$, ${}^4G_{7/2}: 3E_{1/2} + E_{3/2}$ and ${}^2K_{13/2}: 5E_{1/2} + 2E_{3/2}$. Corresponding sets of the transitions are $3\pi\sigma + 2\sigma$, $3\pi\sigma + \sigma$ and $5\pi\sigma + 2\sigma$. According to the observed polarizations of the absorption lines (Fig. 10) and to the separate position of the E1-E5 lines it is logical to refer them to the ${}^4G_{9/2}$ multiplet (Table 3). It is difficult to separate two other multiplets in the F band (Fig. 10).

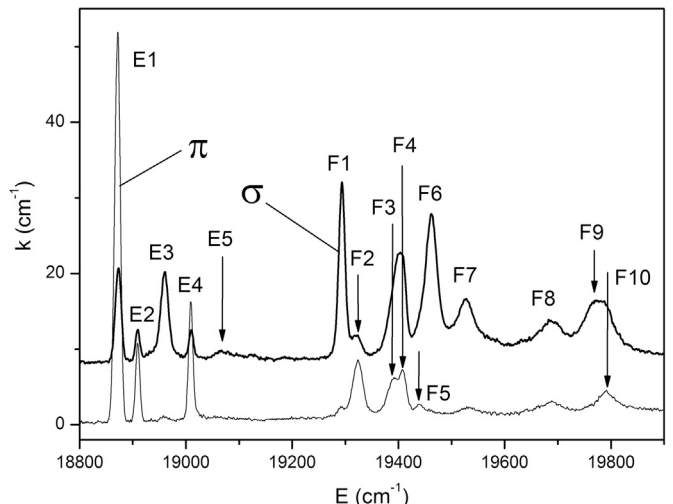


Fig. 10. Polarized absorption spectra of the ${}^4I_{9/2} \rightarrow {}^4G_{9/2} + {}^4G_{7/2} + {}^2K_{13/2}$ transitions (E+F bands) at $T=2$ K.

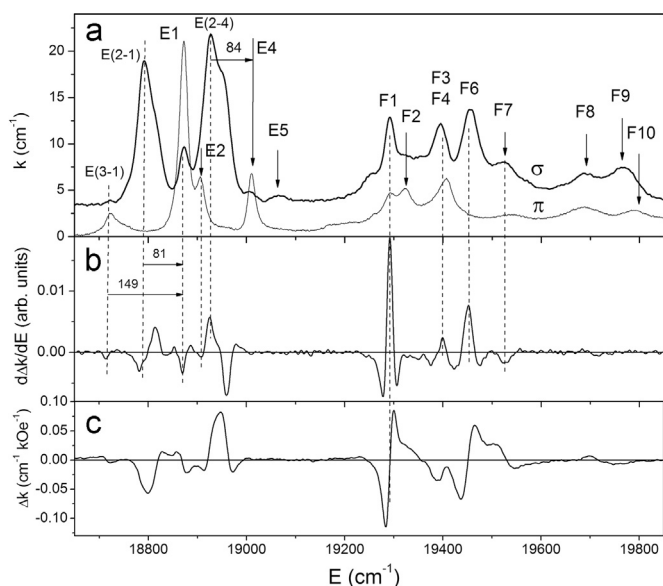


Fig. 11. Polarized absorption spectra (a), the first derivative of MCD (b) and MCD spectra (c) of the ${}^4I_{9/2} \rightarrow {}^4G_{9/2} + {}^4G_{7/2} + {}^2K_{13/2}$ transitions (E+F bands) at $T=90$ K.

Additionally, one σ -polarized line of the transition into the $E_{3/2}$ state is not observed in this band. Signs of $\Delta\omega_0$ (Δg_C) were found (where it was possible) from the $d\Delta k/dE$ function (Fig. 11). It was possible to find values of $\Delta\omega_0$ (Δg_C) only for the lines F1 and F6 (see Table 3). Necessary amplitudes of absorption lines were found as a result of decomposition of the absorption spectrum into the Lorentz components. The F1 state was identified as $M_J=11/2$ (${}^2K_{13/2}$) state since only in this case the theoretical Δg_{CM} is positive and is larger than the measured one.

All results obtained above require some comments. Experimentally observed linear polarizations of lines and symmetry of states are unambiguously connected via selection rules of Table 1. CF mixes states with the same symmetry and so it does not violate selection rules for the linear polarizations of transitions. The situation for the circular polarizations is more complicated. Axially symmetric CF mixes states with the same crystal quantum number μ . However, numbers M_J of the different signs can correspond to the states with the same μ (see Eq. (1)). Consequently, transitions with the participation of such states will have opposite circular polarizations, since the splitting in the magnetic field occurs according to M_J , but the polarization of transitions is governed by the number μ (see Eq. (2)). Majority of the experimentally found $\Delta\omega_0$ (Δg_C) correspond by sign and even by value to the supposed $|J, \pm M_J\rangle$ functions (Table 3), but there are some transitions which contradict to them. This contradiction for the $E_{1/2}$ excited states can be due to the mixing of states with the same number $\mu = \pm 1/2$ and different values and signs of M_J , which give different signs of $\Delta\omega_0$. Additional contribution into the discrepancies can give the mixing of the close manifolds which present in the S, A, D, E and F bands. Such explanation is not suitable for the transitions Gr1 ($J = \pm 5/2, \mu = \mp 1/2 \rightarrow E_{3/2}$), since all these transitions should have negative $\Delta\omega_0$ (Fig. 1). However, if we take into account, that the ground state Gr1 is also a mixture of states with the different M_J , then the same explanation of the discrepancy will be possible.

Positions of states of the ground multiplet found from the different transitions are a little different (see Figs. 3, 5, 7, 9, 11), i.e., the electron transition influences on the local properties of the crystal not only in the excited state but in the initial state as well. In Table 3 the average values are given. Indeed, electron transitions occur due to mixing of initial and final states by the time dependent perturbation caused by the electromagnetic wave. In

conclusion it is worth noting that the above consideration refers to the paramagnetic state of the crystal. In the magnetically ordered state the exchange splitting appear additionally to the CF splitting. The influence of the exchange interaction on the absorption spectra and on the electron states will be considered later.

5. Summary

Polarized absorption spectra and MCD spectra of $\text{Nd}_{0.5}\text{Gd}_{0.5}\text{Fe}_3(\text{BO}_3)_4$ single crystal were measured in the range of $10000\text{--}21000\text{ cm}^{-1}$ and at temperatures $2\text{--}300$ K. In the paramagnetic state of the crystal, the $4f$ states of the Nd^{3+} ion were identified in terms of the irreducible representations and in terms of the $|J, \pm M_J\rangle$ wave functions of the free atom. Basing on this wave function approximations, the Landé factors of the $4f$ states and the changes of the Landé factor during the $f\text{--}f$ transitions were calculated. With the help of the absorption and MCD spectra the changes of the Landé factor during a number of the $f\text{--}f$ transitions were found experimentally. In the majority of cases the experimentally found values are close to the theoretically predicted ones. The discrepancies, observed in some cases, can be accounted for by the mixing of the $|J, \pm M_J\rangle$ states with the different M_J but with the same crystal quantum number μ in the CF.

Acknowledgments

The work was supported by the President of Russia Grant No. Nsh-2886.2014.2.

References

- [1] D. Jaque, J. Alloy. Compd. 323–324 (2001) 204.
- [2] M. Huang, Y. Chen, X. Chen, Y. Huang, Z. Luo, Opt. Commun. 208 (2002) 163.
- [3] X. Chen, Z. Luo, D. Jaque, J.J. Romero, J.G. Sole, Y. Huang, A. Jiang, C. Tu, J. Phys.: Condens. Matter 13 (2001) 1171.
- [4] A.K. Zvezdin, S.S. Krotov, A.M. Kadomtseva, G.P. Vorob'ev, Yu.F. Popov, A.P. Pyatakov, L.N. Bezmaternykh, E.A. Popova, Pis'ma v ZhETF 81 (2005) 335 [JETP Lett. 81 (2005) 272].
- [5] A.K. Zvezdin, G.P. Vorob'ev, A.M. Kadomtseva, Yu.F. Popov, A.P. Pyatakov, L.N. Bezmaternykh, A.V. Kuvardin, E.A. Popova, Pis'ma v ZhETF 83 (2006) 600 [JETP Lett. 83 (2006) 509].
- [6] F. Yen, B. Lorenz, Y.Y. Sun, C.W. Chu, L.N. Bezmaternykh, A.N. Vasiliev, Phys. Rev. B 73 (2006) 054435.
- [7] R.P. Chaudhury, F. Yen, B. Lorenz, Y.Y. Sun, L.N. Bezmaternykh, V.L. Temerov, C. W. Chu, Phys. Rev. B 80 (2009) 104424.
- [8] A.M. Kadomtseva, Yu.F. Popov, G.P. Vorob'ev, A.P. Pyatakov, S.S. Krotov, P.I. Kamilov, V.Yu Ivanov, A.A. Mukhin, A.K. Zvezdin, L.N. Bezmaternykh, I. A. Gudim, V.L. Temerov, Fiz. Nizk. Temp. 36 (2010) 640 [Low Temp. Phys. 36 (2010) 511].
- [9] J.C. Joubert, W. White, R. Roy, J. Appl. Cryst. 1 (1968) 318.
- [10] J.A. Campá, C. Cascales, E. Gutiérrez-Puebla, M.A. Monge, I. Rasines, C. Ruíz-Valero, Chem. Mater. 9 (1997) 237.
- [11] S.A. Klimin, D. Fausti, A. Meetsma, L.N. Bezmaternykh, P.H.M. van Loosdrecht, T.T.M. Palstra, Acta Crystallogr. B 61 (2005) 481.
- [12] E.P. Chukalina, L.N. Bezmaternykh, Fiz. Tverd. Tela 47 (2005) 1470 [Physics of the Solid State, 47 (2005) 1528].
- [13] A.M. Kadomtseva, Yu.F. Popov, G.P. Vorob'ev, A.A. Mukhin, V.Yu. Ivanov, A.M. Kuz'menko, A.S. Prokhorov, L.N. Bezmaternykh, V.L. Temerov, I.A. Gudim, in Proceedings of the XXI International Conference "New in Magnetism and Magnetic Materials," Moscow, 2009, p. 316.
- [14] A.V. Malakhovskii, E.V. Eremin, D.A. Velikanov, A.V. Kartashev, A.D. Vasil'ev, I. A. Gudim, Fiz. Tverd. Tela 53 (2011) 1929 [Phys. Solid State 53 (2011) 2032].
- [15] M.N. Popova, E.P. Chukalina, T.N. Stanislavchuk, B.Z. Malkin, A.R. Zakirov, E. Antic-Fidancev, E.A. Popova, L.N. Bezmaternykh, V.L. Temerov, Phys. Rev. B 75 (2007) 224435.
- [16] A.V. Malakhovskii, A.L. Sukhachev, A.A. Leont'ev, I.A. Gudim, A.S. Krylov, A. S. Aleksandrovsky, J. Alloy. Compd. 529 (2012) 38.
- [17] A.V. Malakhovskii, S.L. Gnatchenko, I.S. Kachur, V.G. Piryatinskaya, A. L. Sukhachev, V.L. Temerov, JMMM 375 (2015) 153.
- [18] A.V. Malakhovskii, S.L. Gnatchenko, I.S. Kachur, V.G. Piryatinskaya, A. L. Sukhachev, I.A. Gudim, J. Alloy. Compd. 542 (2012) 157.
- [19] A.D. Balaev, L.N. Bezmaternykh, I.A. Gudim, V.L. Temerov, S.G. Ovchinnikov, S.

- A. Kharlamova, J. Magn. Magn. Mater. 258–259 (2003) 532.
- [20] A.L. Sukhachev, A.V. Malakhovskii, I.S. Edelman, V.N. Zabluda, V.L. Temerov, I. Ya Makievskii, J. Magn. Magn. Mater. 322 (2010) 25.
- [21] M.A. El'yashevitch., Spectra of rear earths, Moskow (1953) (in Russian).
- [22] A.V. Malakhovskii, A.L. Sukhachev, A. Yu. Strokova, I.A. Gudim, Phys. Rev. B 88 (2013) 075103.
- [23] W.T. Carnall, P.R. Fields, B.G. Wybourne, J. Chem. Phys. 42 (1965) 3797.
- [24] G.H. Dieke., Spectra and Energy Levels of Rare Earth Ions in Crystals, Interscience Publishers, New York, London, Sydney, Toronto, 1968.